Numerical simulation for the flow structures following a three-dimensional horizontal forward-facing step channel

J.G. Barbosa Saldaña, P. Quinto Diez, F. Sánchez Silva, and I. Carvajal Mariscal
SEPI-ESIME-IPN,
LABINTHAP, Unidad Profesional Adolfo Lopez Mateos,
Mexico City, Mexico.

Recibido el 8 de septiembre de 2005; aceptado el 16 de marzo de 2007

A numerical code based on the finite volume discretization technique is developed to simulate flow structures following a three-dimensional horizontal forward-facing step. The link between the pressure distribution and velocity field are made by using the SIMPLE algorithm. A rectangular channel encloses the forward-facing step such that the expansion ratio (ER) and the aspect ratio (AR) are equal to two and four respectively. The total channel length in the stream-wise direction is equal to 60 times the step height and the step edge is located 20 times the step height downstream from the channel inlet. At the channel inlet the flow is considered to be a three-dimensional, fully developed flow. Results for the reattachment line, the separation line, as well as for velocity profiles at different planes for different Reynolds are presented.

Keywords: Numerical simulation; three dimensional; forward-facing step; laminar flow.

En este trabajo se presentan los resultados de la simulación numérica por medio de la técnica de discretización de los volúmenes finitos de las estructuras de flujo tridimensional en un ducto rectangular con un escalón al frente. Se emplea el algoritmo SIMPLE para asociar la distribución de presión y el campo de velocidad dentro del dominio computacional. El ducto que se propone es de forma rectangular y encierra un escalón, de tal forma que la relación de expansión y la relación de aspecto son iguales a dos y cuatro respectivamente. La longitud total del canal en la dirección principal del flujo es igual a 60 veces la altura del escalón, mientras que la orilla del escalón se localiza a una distancia igual a 20 veces la altura del mismo corriente abajo de la entrada del canal. A la entrada se considera que el flujo es tridimensional y completamente desarrollado. Resultados de la línea de reacomodo, línea de separación, así como perfiles de velocidad a diferentes planos dentro del ducto se presentan para diferentes parámetros de Reynolds.

Descriptores: Simulación numérica; tres dimensiones; ducto con escalón al frente; flujo laminar.

PACS: 02.30.Cb; 83.50.Ha; 02.70.Bf; 02.30.Jr

1. Introduction

Separation and reattachment flow is a phenomenon that is found in several industrial devices such as in pieces of electronic cooling equipment, cooling of nuclear reactors, cooling of turbine blades, flow in combustion chambers, flow in vertical plates with ribs, flow in wide angle diffusers, and valves, etc. In other situations, the separation is induced in order to produce more favorable heat transfer conditions as in the case of compact heat exchangers, and even more for understanding the onset of transition to turbulence in natural and mixed convection.

In the last decade, several numerical studies have been conducted to achieve a better knowledge and understanding of the hydrodynamics of the separated flow. In this aspect, the backward-facing step has been the central objective for several studies; and even more, this problem is considered to be a benchmark problem for validating numerical codes and procedures [1,2]. On the other hand, the configuration of a forward-facing step has been investigated much less than the backward-facing step.

Stuer *et al.* [3] mentioned in their publication that very little has been published regarding the laminar separation over a forward-facing step, and neither its topology nor its recirculation zones are known in a predictable form. Abu Mulaweh [4] reports that the phenomenon of convection over the forward-facing step has not been studied due to its complexity. He concludes that, depending on the magnitude of the flow Reynolds number, one or two flow-separation regions may develop adjacent to the step.

Some authors had conducted their researches to analyze the flow passing a forward-facing step. Ratish and Naidu [5] developed a stream function-vorticity formulation for solving the two-dimensional Navier-Stokes equations for laminar flow. In their publication, they did not include the geometrical factors for the computational domain, making their results difficult for being reproduced. In a similar way, Houde *etal.* [6] used a stream-function vorticity formulation for designing a discrete artificial boundary condition for solving the Navier-Stokes equations, to simulate the steady two-dimensional laminar flow problem following a forward-facing step. They implemented a second-order difference scheme to numerically solve the problem. In their study, they present figures showing a re-circulation zone at the step corner, and also a flow separation from the bottom wall after the forward facing step. Even though their results presented an excellent agreement with previous results reported in the literature, their approximation is for a two-dimension problem and cannot be useful for validating the results in this work. Others authors had conducted their studies for the forward-facing step geometry to analyze the mixed convective flow in vertical plates [7] or for studying the mixed convective flow

in a two-dimensional channel for assisting and opposing flow as presented by Abu-Mulaweh and his researching group in several publications [8-10]. Although an important effort in analyzing the flow passing a forward-facing step has been made, most of the studies are limited to the two-dimensional case. Some of the reasons for reducing the problem to a two-dimensional case are the amount of computational resources needed to simulate a three-dimensional flow as well as the problems associated with the convergence rate when numerically simulating a separated flow.

The importance of studying the flow passing a forward-facing step is described by Stuer *et al*. [3] and Ravindran [11]. They mentioned applications that enhance heat transfer and flow mixing rates, flows over obstacles such as buildings, and cooling of electronic equipments, as well as in the control of fluid flow for designing fluid dynamical systems. Even though the applications before mentioned are related to turbulent flow, in this publication the results are presented for the laminar regime as a first stage in this research. In this sense, the results could serve as a first approximation in understanding the separation problem in a forward-facing step and then to set up the numerical procedure to extrapolate it and numerically simulate turbulent flow applications.

In this paper, the analysis for the three-dimensionality of the laminar airflow through a three-dimensional horizontal forward facing step is the objective, and then results for the reattachment, separation and main-stream velocity profiles will be presented in later sections.

2. Model description and numerical procedure

The airflow over a three-dimensional horizontal forward-facing step was numerically simulated via a finite volume discretization technique. The channel aspect ratio and expansion ratio were fixed in relation to the step height ($s = 0.01$ m) as AR = 4 and ER = 2, respectively. The step is located 20 times the step height downstream from the channel inlet ($l = 20$ s), and the total channel length is equal to 60 times the step height ($L = 60$ s). The geometry is presented in Fig. 1.

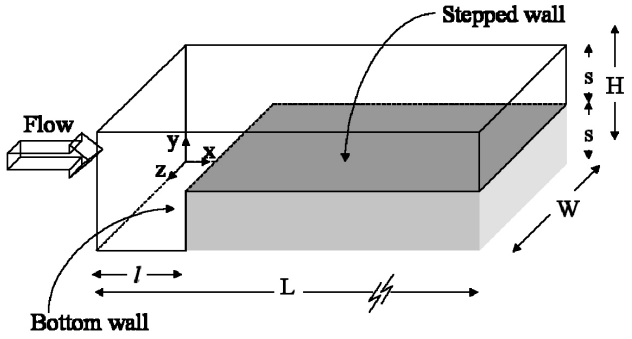

FIGURE 1. Computational domain for the forward-facing step.

At the channel entrance, the airflow was treated as a fully developed flow according to the correlation presented by Shah and London [12]. The no-slip condition was applied at the duct walls, including the stepped wall, and the thermo-physical properties inside the computational domain were assumed to be constants and evaluated at the ambient temperature T_0. The fluid flow problem is considered to be steady state. Hence, the mass conservation and the momentum equations governing the phenomenon are reduced to the following forms [2]:

Continuity Equation:

$$\nabla \cdot \vec{V} = 0 \tag{1}$$

Momentum Equation:

$$\vec{V} \cdot \left(\nabla \vec{V}\right) = -\frac{1}{\rho}\nabla p + \frac{1}{Re}\nabla \cdot \left(\nabla \vec{V}\right) \tag{2}$$

The boundary conditions for the computational domain were established as follow:

$$0 \le x \le L, \quad 0 \le z \le W \quad \begin{cases} y = 0 \\ y = H \end{cases} \{\phi = \phi^*,$$

$$0 \le x \le L, \quad 0 \le y \le H \quad \begin{cases} z = 0 \\ z = W \end{cases} \{\phi = \phi^*,$$

$$0 \le y \le H, \quad 0 \le z \le W \quad \begin{cases} x = 0 \begin{cases} \text{Fully developed} \\ \text{flow [12],} \end{cases} \\ x = L \left\{ \left.\dfrac{\partial \phi}{\partial x}\right|_{x=L} = 0, \right. \end{cases}$$

where $\phi = u, v, w$, and p.

A FORTRAN code was developed to numerically study the problem stated. A finite volume discretization technique was implemented for discretizing the momentum equations inside the computational domain. The SIMPLE algorithm is utilized for linking the velocity and pressure distributions in the iterative procedure. At the final step of every iteration, the velocity field and pressure distribution are corrected and updated to reach convergence as described by Patankar [14]. The power law scheme was utilized to represent the convection-diffusion term at the control volume interfaces [14]. Velocity nodes were located at staggered locations in each coordinate direction, while pressure and other scalar properties were evaluated at the main grid nodes [15]. At the channel exit, the natural boundary conditions $[(\partial\phi/\partial x)|_{x=L} = 0]$ were imposed for all the variables [16]. In addition, the overall mass flow in and out of the computational domain were computed and its ratio was used to correct the outlet velocity at the channel exit [16].

To simulate the solid block inside the domain, a very high diffusion coefficient for the momentum equations was chosen (μ=10^{50}). At the solid-fluid interface, the diffusion coefficients where evaluated by a weighted harmonic mean of the properties in neighboring control volumes as described by Patankar [14].

A combination of the line-by-line solver and the tri-diagonal matrix algorithm was used for each plane in x-, y-,

and z-coordinate directions to compute the velocity and pressure inside the computational domain. Under-relaxation for the velocity components ($\alpha_u = \alpha_v = \alpha_w$=0.4) and pressure ($\alpha_p$=0.4) were imposed in order to guarantee convergence. Convergence for the solution was declared when the normalized residuals for the velocity components and pressure were less than 1×10^{-8} [16].

A non-uniform grid size was considered for solving the numerical problem. In this sense, at the solid walls and at the edge of the forward-facing step the grid was composed of small-size control volumes ($\min_{zcv}$=1.071×10^{-4}m, $\min_{xcv}$=1.71×10^{-4}m $\min_{ycv}$=2×10^{-4}m) and the control volume size increased far away from the solid walls. The grid size was deployed by means of a geometrical expansion factor, so that each control volume is a certain percentage larger than its predecessor. A detailed description of the grid generation can be found in Barbosa, 2005 [17].

The grid independence study was conducted by using several grid densities for a Reynolds number (Re=800) based on the step height. The location at the central plane in the span-wise direction (z/W=0.5) where the stream-wise component of the wall shear stress is zero was monitored to declare grid independence. A grid size of 150:40:40 does not represent an important variation when compared with a 180:40:40 grid size. Hence, the former was proposed for the productive runs.

Table I summarizes the results for the grid independence study. It was observed that increasing the number of nodal points in the transverse (y-coordinate) and span-wise (z-coordinate) directions does not affect the numerical results.

Once grid independence was established, the second step was to find a procedure to validate the numerical code. A direct validation was not possible because there is no published information dealing with the three-dimensional fluid flow problem through a forward-facing step. Then, it was observed that the difference in the numerical implementation between the backward- and forward-facing steps is the location of the block (step). The former refers to a step at the channel's inlet, while the latter one refers to a step and the channel's exit. Hence if the numerical procedure is validated for the backward facing step, it can be useful for solving the forward-facing step problem. In this sense, the forced convective flow through a three-dimensional horizontal backward-facing step was studied and simulated with the same numerical technique, and the results were presented by Barbosa *et al.* [18]. It was found that the numerical predictions using the code presented errors of less than 2% when compared with the experimental published data, thus validating the code for the case of the backward-facing step, and then its application for a forward-facing step. Figure 2 presents a comparison for the x_u-line (to be defined in the next section) obtained with the numerical data and the experimental data obtained by Armaly *et al.* [19]. More information about the validation problem may be found in previous work published by the authors [17,18].

TABLE I. Grid independency study

Grid size x-y-z	Position at the central plane z=0 where τ_{xz}=0	% Difference
180:40:40	0.1820	
150:40:40	0.1812	0.44
150:40:60	0.1816	0.2197
150:60:40	0.1818	0.1098
120:40:40	0.1870	2.75

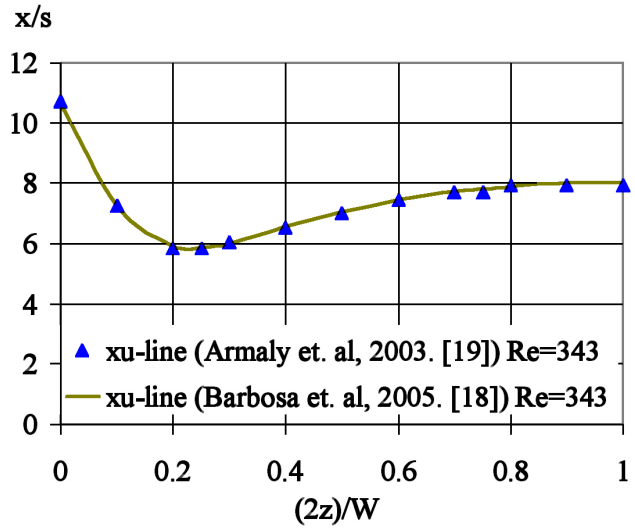

FIGURE 2. x_u-line numerical validation [17].

3. Numerical results and discussion

The numerical study presented in this work considers the flow through a forward-facing step channel for three different Reynolds numbers (Re=200, 400 and 800). The Reynolds number is based on the bulk velocity at the duct entrance (U_b) and twice the channel's step height (H=2s). The coordinate origin for the geometry was placed according to Fig. 1.

A common concept to characterize the separated and reattached flow phenomenon is the end of the re-circulation zone or the point where the wall shear stress is equal to zero. As mentioned by Nie and Armaly [20], for a three-dimensional backward-facing step there is a series of points along the span-wise direction where the wall shear stress is equal to zero. The collection of these points is called the x_u-line and is used to delimit the re-circulation zone along the span-wise direction. Numerically this line is defined as the point in the mainstream flow direction where the u-velocity component changes its value from positive to negative or vice versa.

In a similar way, for the case of the forward-facing step, a re-circulation zone is developed adjacent to the bottom wall and upstream from the step. The line that delimits the starting point for this zone will be referred to as the x-line or separation line, and its distribution along the span-wise direction is presented in Fig. 3 for the three different study cases.

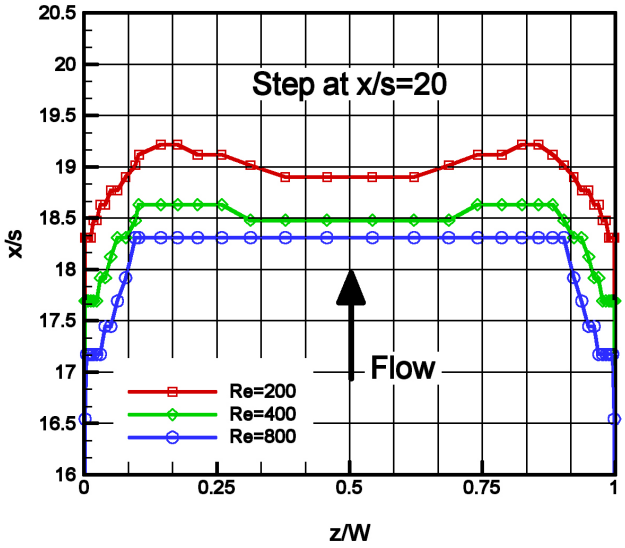

FIGURE 3. Separation line before the step and adjacent to the bottom wall (x-line).

A symmetry behavior for the x-line with respect to the span-wise direction is observed for the three study cases. The flow separation occurs in an earlier position as the Reynolds number is increased, as can be observed in Fig. 3. According to Schlichting and Gersten [21], the separation is governed by the pressure gradient and the friction along the wall. In this regard, it can be considered that the pressure drop and the friction along the wall are larger for higher Reynolds numbers. Figure 3 also reveals that, near the sidewalls, the lowest x/s values for the x-line are found. This behavior could be explained due to the presence of the sidewalls and the no-slip condition imposed for the numerical simulation.

According to White [22], the flow passing the step edge is separated, and somewhere downstream it will be reattached. This phenomenon was observed in the numerical simulation and the results for Re=200, Re=400 and Re=800 are presented in Figs. 4a, 4b and 4c, respectively. In these figures the colored zones represent regions where the u-velocity component has negative values, while the cleared zones are associated with positive values for the mainstream velocity component (u-velocity). The x-axis is shortened to show the vicinity, on the step. Values for x less than 0.2 (x<0.2) represent the bottom wall, whereas the gray zone is used to represent the stepped wall (x>0.2). Here the values for the u-velocity component correspond to the horizontal plane nearest to the bottom wall and stepped wall respectively.

As can be appreciated in Fig. 4, the amplitude of this zone in the main flow direction is of the order of a few centimeters, and the trend for the re-circulation zone is similar for the three study cases. The largest re-circulation zone corresponds to the highest Reynolds (Fig. 4c) while the smallest re-circulation zone belongs to Re=200 (Fig. 4a).

In the three cases, two re-circulation zones can be clearly identified. One before the step (x<0.2) and the other over the stepped wall (x>0.2). Figures 4b and 4c show that, before the step and along the span-wise coordinate, there is a zone for the positive u-velocity component. This zone is not presented all along the span-wise direction for Re=200. However, it can be observed that, at the corners of the step and the sidewalls, there are localized zones for the positive u-velocity component. According to the mass conservation and the no-slip-no-penetration imposed boundary conditions, these zones must be zones of high three-dimensional flow.

For Re=800, a zone of positive values (white zone) can be appreciated for the u-velocity component inside the re-circulation zone located upstream from the step. This particular behavior is not presented at Re=200 nor at Re=400.

Figure 4 shows that the starting of the re-circulation zone over the step is almost a straight line. The reason for this particular behavior is related to the fact that the abrupt change in the geometry that produces the separation is located at the same position for the entire span-wise direction (the step edge). However, at the end of this re-circulation zone the line along the span-wise direction delimiting the re-circulation zone presents an irregular line. This could be associated with the development of zones of high three-dimensional flow after the step edge and mainly inside the re-circulation zone that is developing in this zone. As can be appreciated, the delimiting re-circulation zone for Re=800 (Fig. 4c) has more irregularities than the other two cases as a result of higher three-dimensional behavior of the flow in this zone.

In order to have a detailed understanding of this phenomenon, the wall shear stress averaged (τ) over the span-wise direction is plotted along the main flow direction (x) in Fig. 5. As can be appreciated, the wall shear stress presents a similar behavior for the three study cases. At the channel inlet, the flow was considerered to be a fully developed flow, and therefore the horizontal line in the plot. However, in the vicinity of the step (x/L=0.33) the lines present negative values for (τ) associated with the presence of the primary re-circulation zone. At the step edge, the τ-lines present a discontinuity due to the abrupt change in the geometry. After the step edge, the values for the shear stress present high values (redeveloping zone), and then the values have a tendency towards an asymptotic value at the channel's exit.

A zoom for the zone at the vicinity of the step is also presented in Fig. 5. Here fluctuations can be appreciated from positive to negative values for Re=800. This behavior is not too apparent for Re=400, and definitely does not appear for Re=200. The fluctuations just mentioned for Re=800 are associated with the presence of zones with positive values for the u-velocity component before the step as discussed earlier.

At the channel exit, the averaged values for the shear stress tend to an asymptotic value. However, the only values that really approximate to an asymptotic value, and then reach the fully developed conditions, are those for Re=200. This behavior does not occur for Re=400 nor for Re=800, meaning that for these values the channel is not long enough to accommodate fully developed flow, as will be discussed after Fig. 13.

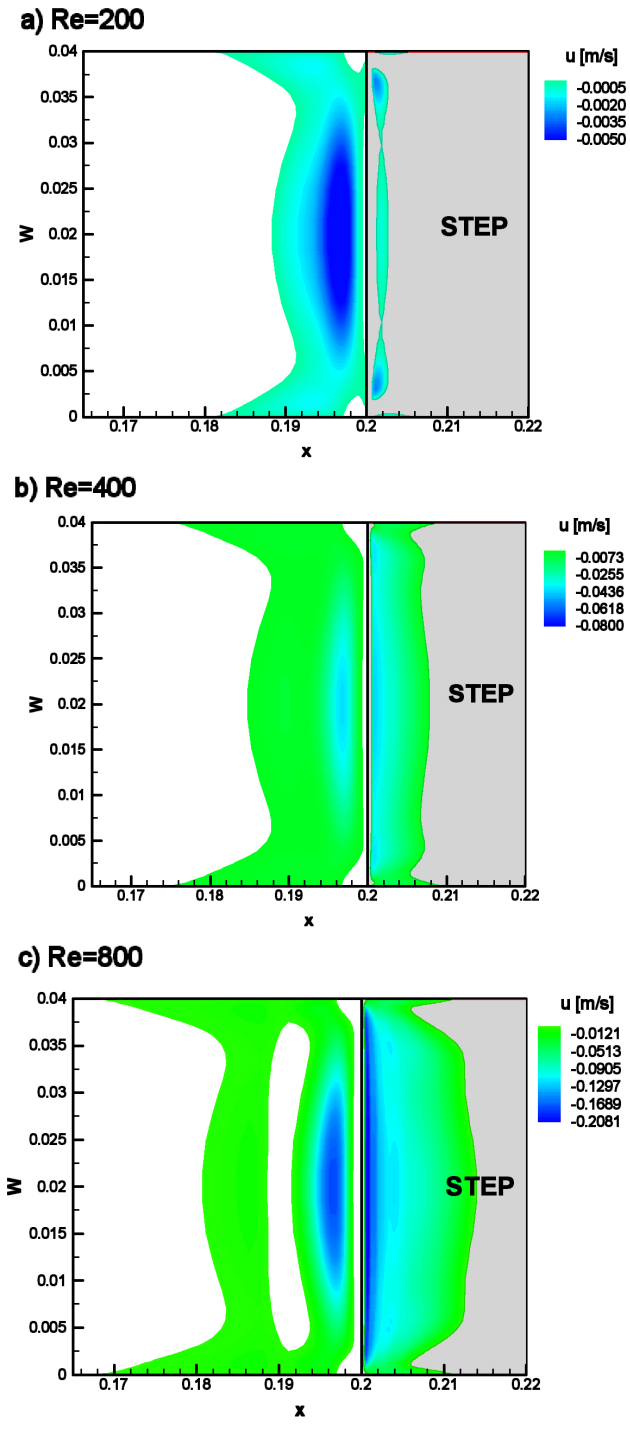

FIGURE 4. Re-circulation in a horizontal plane adjacent to the stepped wall a) Re=200, b) Re=400 c) Re=800.

Figure 6 is intended to present the stream traces along the central plane in the span-wise direction (z/W=0.5) for Re=200. Figure 6a presents a zoom augmentation to detail the flow structures at the edge of the forward-facing step, while Fig. 6b is used to detail the corner at the bottom wall and the step. In both figures the re-circulation zone on the stepped wall and the re-circulation zone on the bottom wall are perfectly defined respectively, while Fig. 6c is used to represent the flow structures at the upper wall. It is also observed from Fig. 6d that once the flow is reattached to the stepped wall it continues developing towards the channel exit.

Figure 7 presents the same flow structures as Fig. 6, but the Reynolds parameter is Re=800.

The flow structures for Re=800 not only present a more complicated vortex inside of the re-circulation zones, but also reveal a larger size of these zones in the x-as well as in the y-coordinate direction. In Fig. 7b, the existence of two vortices inside the re-circulation zone adjacent to the bottom wall and step is found (x<0.2m). Figure 7b shows very clearly the formation of the re-circulation zone adjacent to the step edge. Unlike Fig. 6b, it is observed that, for Re=800, the flow separation occurs closer to the step edge than for Re=200. Similarly, for Re=800 the re-circulation zone over the step is perfectly defined in Fig. 7c, and this effect is less well defined for Re=200 in Fig. 6c.

The stream traces presented in Figs. 6d and 7d for Re=200 and Re=800 respectively, shows that in both cases the flow structures experienced a kind of hydraulic jump at the step edge. In order to illustrate this particular behavior in Figs. 8, 9 and 10, three-dimensional streamlines for Re=200, 400 and 800 into the computational domain respectively are presented. Similarly, these figures show the re-circulation zone in the three-dimensional computational domain.

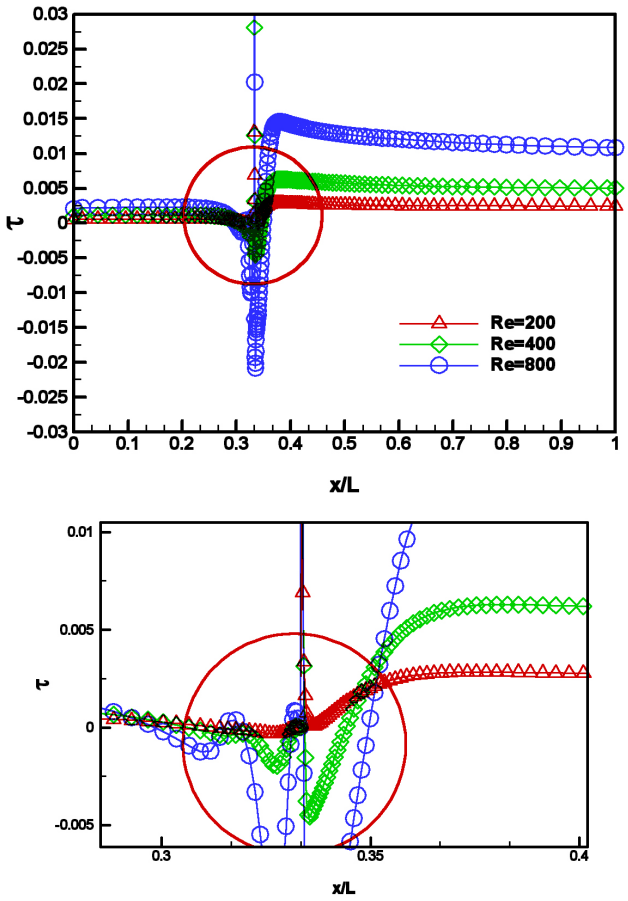

FIGURE 5. Wall shear stress averaged over the span-wise direction.

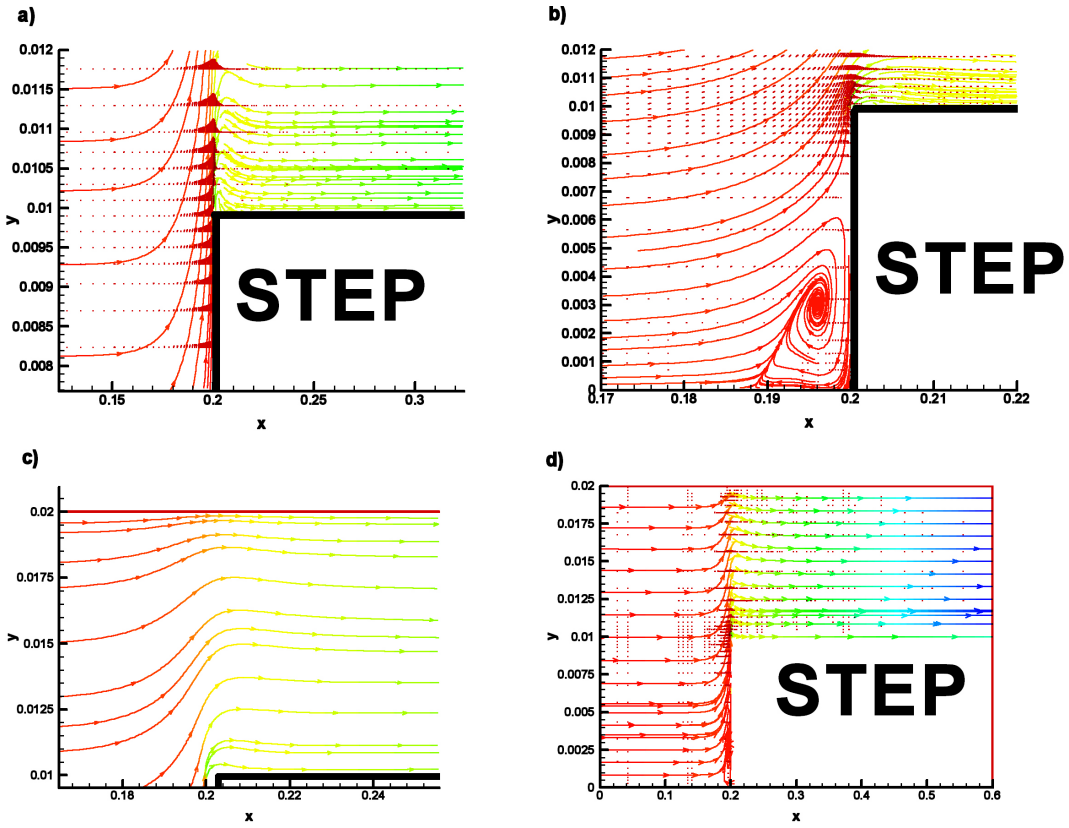

FIGURE 6. Stream traces and pressure contours for Re=200 at the central plane in the span-wise direction (z/W=0.5) a) step edge, b) step corner at the bottom wall, c) step edge and top wall, d) stream traces .

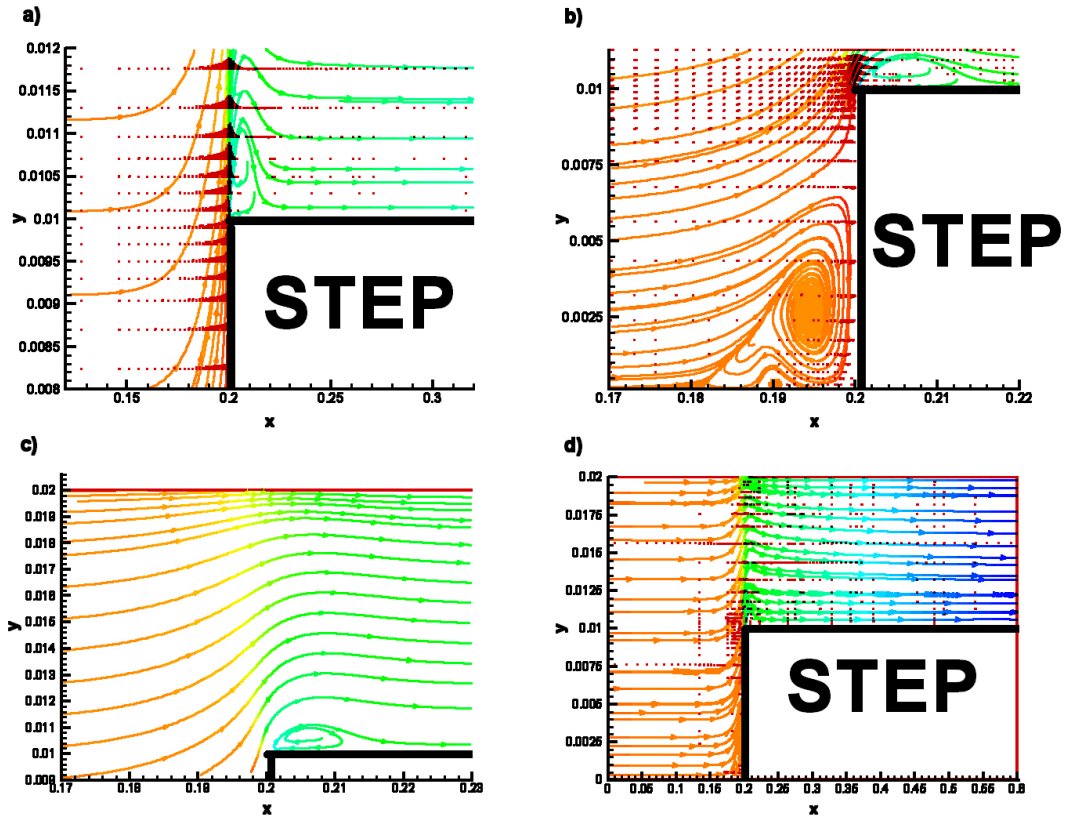

FIGURE 7. Stream traces and pressure contours for Re=800 at the central plane in the span-wise direction (z/W=0.5) a) step edge, b) step corner at the bottom wall, c) step edge and top wall, d) stream traces.

The above mentioned figures perfectly show the hydraulic jump at the step edge. The phenomenon is more evident as the Reynolds number is increased. After this point, the stream traces show that the flow continues developing towards the channel exit. Special attention should be paid to Fig. 10. Here it is observed that some stream lines came from the channel inlet and jump the step, but their momentum is too large that they impact against the top wall and then are displaced to the stepped wall and towards the channel exit. In comparison with the streamlines for Re=400 and Re=200, it is observed that the lines coming from the channel inlet jump the step moving to the top wall and then remain in the upper part of the channel. The difference in this behavior should be associated with the higher momentum for a higher Reynolds.

Figures 8, 9 and 10 also illustrate the re-circulation zones inside the computational domain for the three Reynolds studied. It is observed that, as Reynolds increases, the presence of re-circulation zones become more evident, having larger extensions of negative u-velocity component in the vertical, axial and transversal coordinate direction.

Finally, to give more information of the flow structures, some plots for the u-velocity at constant z- and x-planes are discussed.

In Fig. 11, the u-velocity profile at the central plane in the span-wise for an x-constant plane before the step is presented. In order to have a better appreciation of the re-circulation zone, the vertical axis of the figure is shortened, and only the values near the bottom wall are plotted. In this figure, the negative values for the u-velocity component are evidence for everything discussed before referring to the re-circulation zone adjacent to the bottom wall before the step. Close to the bottom wall, for Re=800 a zone of positive values for the u-component is found. This particularity indicates that the re-circulation zone for Re=800 does not finish at the step, but at some previous point, as mentioned earlier. Another implication is that the v-velocity component at this zone must have positive values in order to satisfy continuity. On the other hand, for Re=200 and Re=400 the negative values for the u-velocity component start at the bottom wall.

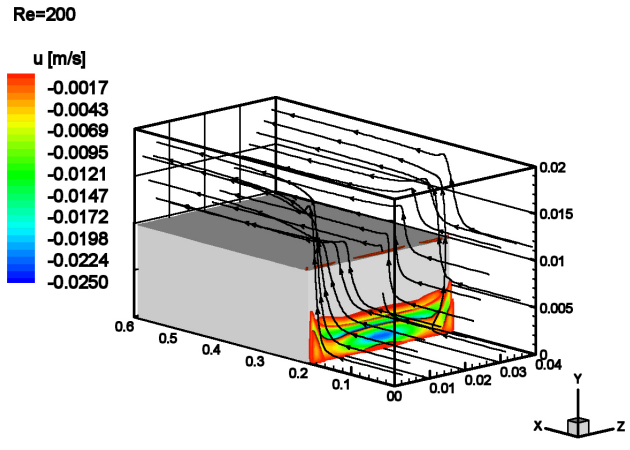

FIGURE 8. Streamlines and re-circulation zones for Re=200.

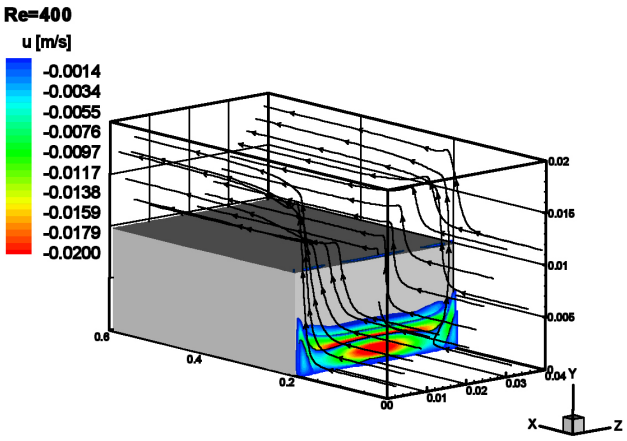

FIGURE 9. Streamlines and re-circulation zones for Re=400.

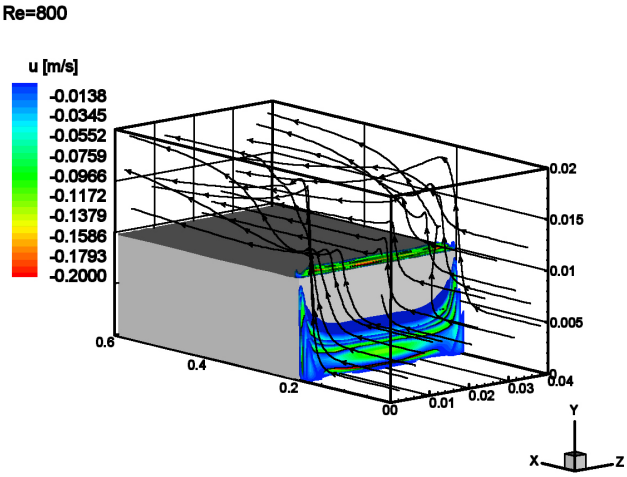

FIGURE 10. Streamlines and re-circulation zones for Re=800.

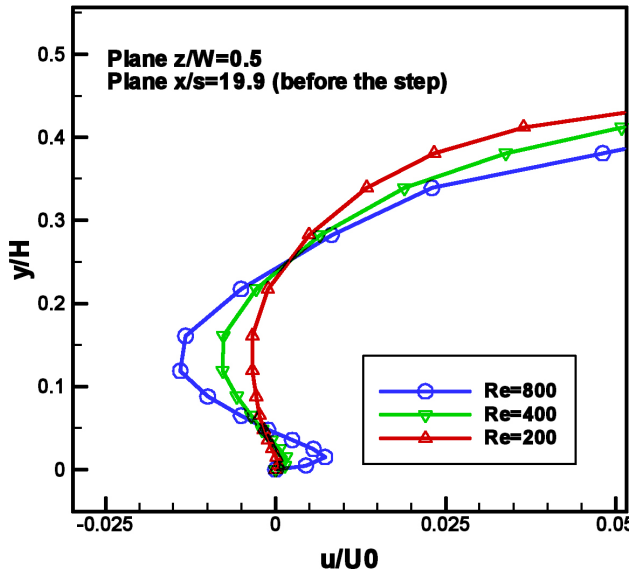

FIGURE 11. u-velocity profile at the central span-wise plane and x/s=19.9.

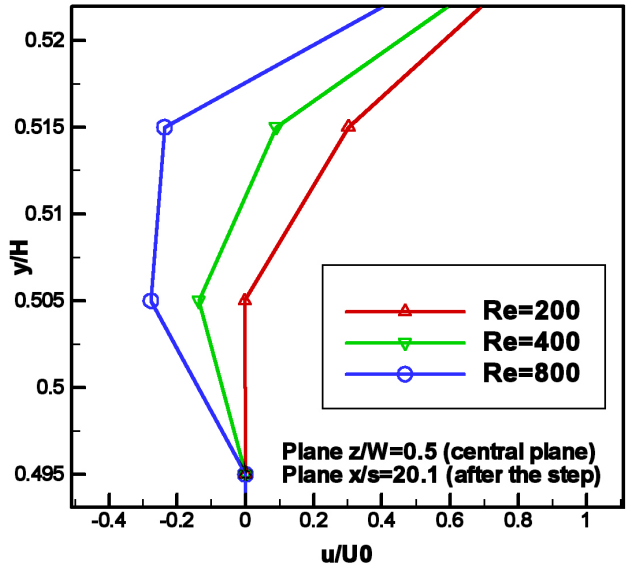

FIGURE 12. u-velocity profile at the central span-wise plane and x/s=20.1.

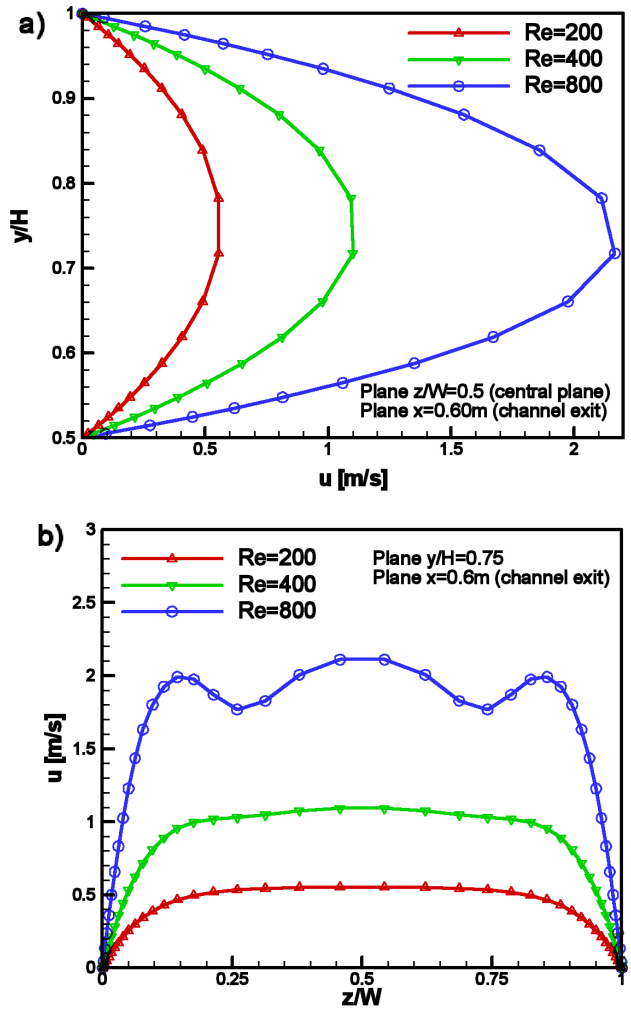

FIGURE 13. u-velocity profile at the central span-wise plane (z/W=0.5) and channel exit (x/L=1).

Figure 12 shows the u-velocity profile for the central plane in the span-wise direction for a constant x-plane just passing the step edge. The u-component negative values for Re=800 and Re=400 indicate that the flow separation along the stepped wall starts earlier than for Re=200. This effect was discussed above.

The u-velocity profile at the channel exit for the middle plane in the span-wise direction is presented in Fig. 13a, while Fig 13b is used to present the u-velocity component at the channel exit and a y/H=0.75 plane. Here it is evident that the channel is long enough to accommodate fully developed flow for Re=200, due to the fact that the velocity profile is parabolic in the vertical coordinate as well as in the transverse coordinate. However, for Re=800, there are slight differences from the parabolic profile in the vertical coordinate, and it definitely presents a no-parabolic profile in the transverse direction, meaning that at the channel exit the flow is not a fully developed flow.

4. Conclusions

The numerical results for simulating airflow through a horizontal channel with a forward-facing step were presented for three different Reynolds parameters.

The flow structures showed that the flow is separated and reattached in two different regions. One before the step adjacent to the bottom wall and the other is developed adjacent to the stepped wall after the step edge. The size and location of these re-circulation zones depend on the Reynolds parameter. As Reynolds is increased, the re-circulation zones before and after the step increases their size. It is also observed that as Reynolds is increased, the separation flow occurs at earlier positions in the main flow direction.

It was found that, as the Reynolds is increased, more complex flow structures are found and then the flow is strongly three-dimensional.

Although some results in this geometry were presented, it is necessary to continue a methodic study in order to characterize this important phenomenon.

5. Nomenclature

AR	aspect ratio, W/s
ER	expansion ratio, H/s
H	channel height [m]
l	channel inlet, 20s [m]
L	channel total length, 60s [m]
p	pressure [Pa]
Re	Reynolds number $Re = 2\rho U_0 s/\mu$
s	step height [m]
T_0	Ambient temperature [273 K]
V	velocity [m/s]
W	channel width [m]

x	stream wise direction/coordinate
y	transverse direction/coordinate
z	span wise direction/coordinate
min	minimum or smallest
U_o	bulk velocity at the channel inlet
u	stream wise velocity component x-direction
v	vertical velocity component y-direction
w	span wise velocity component z-direction

Greek letters

ϕ	dependent variable
μ	fluid dynamic viscosity (1.81x10^{-5} kg/m-s)
ρ	fluid density (1.205 kg/m^3)

Subscripts

b	bulk
cv	control volume
0	inlet conditions
w	wall conditions

Superscripts

*	starting conditions

1. *Benchmark problems for heat transfer codes*, B.F. Blackwell and D.W. Pepper, (eds), ASME-HTD-222: Anaheim, (1992).
2. P.T. Williams and A.J. Baker, *Int. J. Numerical Methods in Fluids* **24** (1997) 1159.
3. H. Stuer, A. Gyr, and W. Kinzelbach, *Eur. J. Mech. B/Fluids* **18** (1999) 675.
4. H.I. Abu-Mulaweh, "A review of research on laminar mixed convection flow over a backward- and forward-facing steps" *Int. J. of Thermal Sciences* to be published (2003).
5. B.V. Ratish-Kumar and K.B. Naidu, *Applied Numerical Mathematics* **13** (1993) 335.
6. H. Houde, J. Lu, and W. Bao, *J. Computational Physics* **114** (1994) 201.
7. A. Asseban *et al.*, *Optics & Laser Technology* **32** (2000) 583.
8. H.I. Abu-Mulaweh, B.F. Armaly, and T.S. Chen, *J. Thermophys Heat Transfer* **7** (1993) 569.
9. H.I. Abu-Mulaweh, B.F. Armaly, T.S. Chen, and B. Hong, *Proceedings of the 10th International Heat Transfer Conference* **5** (1994) 423.
10. H.I. Abu-Mulaweh, B.F. Armaly, and T.S. Chen, *Int. J. Heat Mass Transfer* **39** (1996) 1805.
11. S.S. Ravindran, *Computer methods in applied mechanics and engineering* **191** (2002) 4599.
12. R.K. Shah and A.L. London, *Laminar flow forced convection in ducts* (Academic Press, New York, 1978).
13. S. Kakac and Y. Yener, *Convective Heat Transfer* (CRC Press, Inc., Boca Raton, 1995).
14. S.V. Patankar, *Numerical heat transfer and fluid flow* (Taylor and Francis, Philadelphia, 1980).
15. K.M. Kelkar and S.V. Patankar, *Computer Physics Communications* **53** (1989) 329.
16. J.G. Barbosa-Saldana, N.K. Anand, and V. Sarin, *Int. J. Heat Transfer* **127** (2005) 1027.
17. J.G. Barbosa Saldana, *Numerical Simulation of Mixed Convection over a Three-Dimensional Horizontal Backward-Facing Step*, Texas A&M University Doctoral Dissertation, College Station, (2005).
18. J.G. Barbosa-Saldana, N.K. Anand, and V. Sarin, *Int. J. of Computational Methods in Engineering Science and Mechanics* **6** (2005) 225.
19. B.F. Armaly, A. Li, and J.H. Nie, *Int. J. Heat and Mass Transfer* **46** (2003) 3573.
20. J.H. Nie and B.F. Armaly, *Int. J. of Heat Transfer* **125** (2003) 422.
21. H. Schlichting and K. Gersten, *Boundary Layer Theory* (Springer, Berlin, 2000).
22. F.M. White, *Mecanica de Fluidos* (McGraw Hill, Ciudad de Mexico, 1999).